Inorganic Chemistry

Forum Article

pubs.acs.org/IC

Ferritin: The Protein Nanocage and Iron Biomineral in Health and in Disease

Elizabeth C. Theil*

Children's Hospital Oakland Research Institute (CHORI), 5700 Martin Luther King Jr. Way, Oakland, California 94609, United States, and Department of Molecular and Structural Biochemistry, North Carolina State University, Raleigh, North Carolina 2765-7622, United States

ABSTRACT: At the center of iron and oxidant metabolism is the ferritin superfamily: protein cages with Fe^{2+} ion channels and two catalytic Fe/O redox centers that initiate the formation of caged $Fe_2O_3{\cdot}H_2O$. Ferritin nanominerals, initiated within the protein cage, grow inside the cage cavity (5 or 8 nm in diameter). Ferritins contribute to normal iron flow, maintenance of iron concentrates for iron cofactor syntheses, sequestration of iron from invading pathogens, oxidant protection, oxidative stress recovery, and, in diseases where iron accumulates excessively, iron chelation strategies. In eukaryotic ferritins, biomineral order/crystallinity is influenced by nucleation channels between active sites and the mineral growth cavity. Animal ferritin cages contain, uniquely, mixtures of catalytically active (H) and inactive (L) polypeptide subunits with varied rates of Fe^{2+}/O_2 catalysis and mineral crystallinity. The relatively low mineral order in liver ferritin, for example, coincides with a high percentage of L subunits and, thus, a low percentage of catalytic sites and nucleation channels. Low mineral order facilitates rapid iron turnover and the physiological role of liver ferritin as a general iron source for other tissues. Here, current concepts of ferritin structure/function/genetic regulation are discussed and related to possible therapeutic targets such as mini-ferritin/Dps protein active sites (selective pathogen inhibition in infection), nanocage pores (iron chelation in therapeutic hypertransfusion), mRNA noncoding, IRE riboregulator (normalizing the ferritin iron content after therapeutic hypertransfusion), and protein nanovessels to deliver medicinal or sensor cargo.

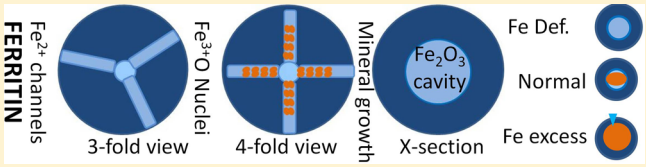

1. INTRODUCTION

Iron, essential for life, is mainly in proteins, but recent studies show selective, coordination binding of Fe^{2+} to RNA; examples include enhanced ribozyme folding/activity[1] and a changed RNA riboregulator conformation in the 5′ untranslated region of animal mRNA that dissociated a protein repressor[2] and enhanced translation factor (eIF-4F) binding.[3] The major iron proteins in humans are globins, hemoglobin and myoglobin, followed by ferritins, and then by a variety of heme and iron−sulfur proteins and iron cofactors bound directly to protein, e.g., ribonucleotide reductase. Ferritin is a superfamily of protein-caged $Fe_2O_3{\cdot}H_2O$ biominerals. They are ancient (in Archaea) and ubiquitous (in marine and terrestrial organisms, both anaerobic and aerobic) and have a rare quaternary structure: folded, polypeptide subunits (four α-helix bundles) that self-assemble into hollow cages; interior cage spaces (biomineral growth cavities) that are ~30% of the cage volume. The cage symmetry is 432 (24 subunit ferritins) or 32 (12 subunit ferritins, often called Dps proteins or mini-ferritins). The amino acid sequences of ferritins vary as much as 80%, although subdomains, such as the Fe^{2+} entry/exit channels, contain highly conserved sequences. Multiple ferritin genes in eukaryotes create tissue-specific combinations of ferritin subunits in the cages, contrasting with bacterial ferritin genes, which encode ferritin subunits for homopolymeric cages synthesized at different times in the culture cycle.[4,5] In animal tissues, including humans, both the ferritin mineral and ferritin protein vary among each tissue and cell type. The crystallinity of ferritin biomineral coincides with variations in the structure of the protein cage.[6] Such cage variations include, in addition to the amino acid sequence, the numbers of catalytically active subunits with nucleation channels (H subunits) and the iron ligands at the active sites, which emphasize protein-based contributions to the ferritin mineral structure.[7] For decades, serum ferritin, normally 0.025% of the total body ferritin, has been used as a clinical marker of iron status; serum ferritin likely originates from cell leakage. Recent awareness of the role of inflammation in altering serum ferritin concentrations complicated the interpretation of serum ferritin as a marker for body iron. The physiology and structure of serum ferritin remain poorly understood and will not be considered further. Briefly described here are the ferritin protein structure and function, the ferritin mineral structure and function, the regulation of ferritin biosynthesis, and the use of ferritin as a therapeutic target in disease.

2. FERRITIN PROTEIN STRUCTURE

Ferritin subunits (Figure 1A,C) spontaneously self-assemble into the native, protein nanocages (Figure 1), although recent

Special Issue: Metals in Medicine and Health

Received: February 24, 2013
Published: October 8, 2013

dx.doi.org/10.1021/ic400484n | *Inorg. Chem.* 2013, 52, 12223−12233

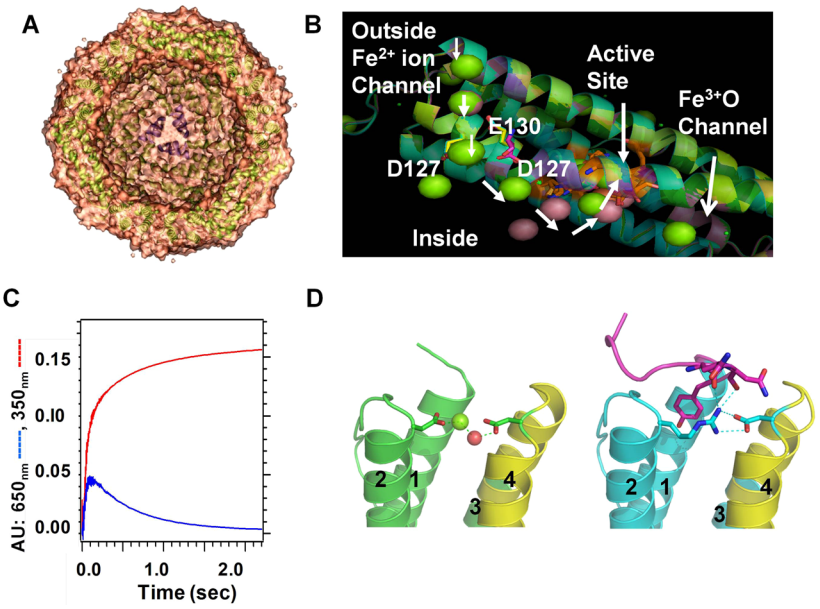

Figure 1. Ferritin protein: (A) X-section of a eukaryotic ferritin protein cage, viewed with a 3-fold symmetry axis pore centered in the mineral growth cavity. (B) Ferritin protein subunit: metal-ion traffic (white arrows) in a; protein cocrystal with Mg^{2+} (green sphere) and Co^{2+} (pink sphere) in the channel at the left. (C) Progress curves of Fe^{2+}/O_2 catalysis: $Fe^{3+}-O-O-Fe^{3+}$ (diferric peroxo, DFP; λ_{max} = 650 nm), blue; $Fe^{3+}O$ (broad absorbance A = 350 nm), red. (D) N-Terminal extension, R72D, left; N-terminus disordered, WT, right; N-terminus, pink; helix numbers = 1–4. Fe^{2+} exit from the ferritin mineral is accelerated in R72D.[11,12] Figure panels contributed by T. Tosha and R. K. Behera, using PDB 3KA4, PDB 3DE1, and Pymol.

engineering approaches are now providing access to single ferritin subunits for study and modification before reassembly.[8] Curvature of the subunit bundles creates a large hollow in the protein cage (Figure 1A). It is the geometry of side-chain interactions at the subunit dimer interfaces that controls ferritin cage self-assembly, based on recent data.[9] The use of a single Fe^{2+} channel to provide a substrate to three diiron catalytic sites, in the three subunits of ferritin cages that form the ion channels, is associated with a Hill coefficient of 3; the underlying protein–protein interaction remains unknown.[10] Each ferritin subunit has an N-terminal peptide extension, which, in eukaryotic ferritins, is a gate for mineral dissolution/Fe^{2+} exit; it is held in place by conserved hydrogen-bonding interactions with residues in the subunit in channels. Gate function was recently identified through the structural disorder induced with amino acid substitution of conserved ion-channel residues (Figure 1D) and the associated increase in the rates of mineral dissolution and Fe^{2+} exit/chelation.[11,12]

Variations in the ferritin primary structure between bacterial and eukaryotic ferritins can be huge, as much as 80%, even though the protein cage structures are similar. Among eukaryotic ferritins, however, the sequence divergence is only 30–40%, allowing animal sequences to identify plant genes.[13] The three-dimensional structural similarities of 12 subunit mini-ferritins (Dps/DLP proteins) and 24 subunit maxi-ferritins escape current bioinformatic analyses of linear ferritin sequences. The ferritin cage structure of Dps proteins was not recognized until the first protein crystal structure of a 12 subunit Dps protein was obtained in *Escherichia coli*.[14] The N- and C- terminal extensions from four ferritin α-helix bundles vary in length and structure. In some mini-ferritins, N-termini are associated with DNA binding and DNA protection, hence the name Dps (DNA protection during stress/starvation). N-Terminal extensions of some mini-ferritins contain short α-helices.[15]

a. Protein Cages. Ferritin protein cages in animals and plants are heteropolymers of ferritin subunits encoded in separate genes. The added level of complexity is critical physiologically because different tissues, e.g., root leaves and seeds in plants and liver spleen, heart, and intestine in animals, synthesize ferritins with different, specific mixtures of subunits. In animals, the different subunit mixtures coincide with different mineral structures[6] and with the accessibility of ferritin iron to iron chelators.[16] A limitation of standard recombinant protein technology for ferritins from plants and animals is the fact that coexpression strategies are required to produce ferritin cages with mixtures of subunits,[17] while most current research uses homopolymeric ferritins. However, as more is learned about homopolymeric recombinant ferritin protein cages, especially of highly conserved sections, readily interpretable experiments with heteropolymeric cages can be designed and executed.

Protein crystallography has been the main source of structural information about ferritins since 1978 because suitable crystals of ferritin are obtained relatively easily. However, recently, a combination of solid-state and solution $^{13}C-^{13}C$ NOESY NMR has provided new information on the functional structure in eukaryotic ferritin protein cages.[18,19] Currently, in the RCSB Protein Data Base, there are 177 structures of 24-subunit ferritins, 48 structures of 24-subunit heme bacterioferritins, and 6 structures of 12-subunit mini-ferritins.

The high α-helix content of ferritin protein cages (>80%) facilitates the use of circular dichroism to study the thermal and solvent stability of protein cages and subdomains in normal and variant cages.[8,20] Protein crowding (increasing osmolarity with soluble proteins to approximate cytoplasmic conditions) partly restores function in unfolded ferritin variants, suggesting possible rescue pathways for abnormally unfolded ferritin in vivo.[11,21] Several novel NMR approaches, both solution,[19,22] are

dx.doi.org/10.1021/ic400484n | *Inorg. Chem.* 2013, 52, 12223–12233

Table 1. Examples of Ligands at 24-Subunit Ferritin Diiron Catalytic Centers (n = 4−24/Cage[a])

	Fe-1	Fe-2	function	ref
Eukaryotic maxi-ferritin: *H. sapiens*/*R. catesbeiana*/*G. max*	E, ExxH	E, QxxA/D/S	substrate and DFP[b]	10, 28−33
Bacterial maxi-ferritin: *E. coli* BFR	E, ExxH	E, ExxH	cofactor and substrate	34, 35
Archeael maxi-ferritin: *P. furiosus*	E, ExxHE	E,QxxE	cofactor and substrate	27, 36
Bacterial mini-ferritin:[c], *B. anthracis* Dps-1	H, HxxE[c]	E, DxxxE	substrate	37−39

[a]In animals, ferritins from different tissues combine different numbers of catalytically inactive (L) and active (H) subunits/cage. In plants, ferritins have multiple type H subunits with different amino acid sequences.[40] In bacteria, ferritins contain only one type of catalytically active (H) subunit at a time, but different ferritins, encoded in separate genes, are synthesized under different conditions.[5,26] [b]DFP (Fe^{3+}−O−O−Fe^{3+}) forms as a transient intermediate at eukaryotic ferritin catalytic centers. [c]In the absence of oxidant, the Fe1 site is empty.

being developed to solve the problems of ferritin function, the first dealing with product release in catalysis and mineral nucleation.

Comparisons of the protein cages of ferritin family members show that they share multipolypeptide, hollow cages, in spite of linear sequences that vary as much as 80%. The polypeptides spontaneously fold into bundles of four α-helices (Figure 1). Ferritin helix bundles deviate from classical polarity, helix 1 (up)/helix 2 (down)/helix 3 (up)/helix 4 (down), because of the very long loop connecting helices 2 and 3. In contrast, ferritin helix bundles are helix 1 (up)/helix 2 (down)/helix 3 (down)/helix 4 (up) (see Figure 1D). Self-assembly of ferritin subunits depends on interfacial geometries conferred by hydrogen bonding that interdigitate long, dimeric helical interfaces.[8] The increased stability gained by cage assembly is illustrated by the midpoint thermal unfolding transition at 40 °C for each subunit bundle, contrasting with 80 °C for the assembled cage.[8]

b. Ion Channels and 3-Fold Symmetry Axes. Trimers of helix 4 form the walls of a single ion channel around the cage 3-fold symmetry axes, which penetrate the ferritin protein cages. The eight ion channels in 24-subunit ferritins have an hourglass shape, are 15 Å long, and assemble around the 3-fold symmetry axes of the cage. Fe^{2+} ions traverse the ion channels during entry for mineral formation and during exit after mineral dissolution.[7,15] Changing tertiary structural interactions in the 3-fold channel can alter ferritin function.[4,11,12,23−25]

c. Catalytic Sites. Ferritin catalytic sites are generally in the middle of each subunit with metal ligands from each of the four α-helices in the bundle; exceptions occur in a few mini-ferritins.[15] The amino acids at the active sites are similar among animals, plants, and microorganisms but not identical (Table 1). Ligand weakness at one of the active sites in most ferritins (Table 1) reflects the release of the catalytic product, $Fe^{3+}O$. An exception is bacterioferritin, where the ligand sets for each iron at the diiron catalytic centers are the same and like those in the diiron oxygenases. In fact, the diiron center in bacterioferritins does, as in diiron oxygenase, retain iron and acts as a cofactor.[26] Given the variations in the amino acid sequence of ferritin cages and the differences among ferritin catalytic site ligands (Table 1) and oxidants (O_2 and/or H_2O) (up 80%), attempts to fit one catalytic mechanism to data on all known ferritins[27] seem premature.

Only in animal ferritins is the number of catalytic sites less than the number of cage subunits because only animals produce catalytically inactive L subunits, lacking both a functional catalytic site and nucleation-channel residues. Tissue-specific differences in the H and L subunit content of ferritin protein cages coincide with tissue-specific differences in the ferritin mineral crystallinity.[6]

d. Postoxidation/Nucleation Channels and the 4-Fold Symmetry Axes. The ferritin $Fe^{3+}O$ channels in 24-subunit ferritins, which terminate around the inner surfaces of the 4-fold cage symmetry axes (Figure 3), were discovered by monitoring the pathway of Fe^{3+} after catalytic reactions with O_2, from the active sites to the mineral growth cavities, with $^{13}C-^{13}C$ NOESY NMR (Figure 3);[19] the amino acids along the postoxidation channel alter DFP kinetics when they are replaced.[4] Restoration rates of the active sites for Fe^{2+} binding are slow and heterogeneous (6−24 h)[41,42] and contrast with the simple, rapid decay of DFP (seconds; Figure 1). However, the long periods of time required for site restoration (turnover) match that required for fluctuations in NMR spectra to return to the original steady state, after the addition of Fe^{2+} in air,[19] and likely reflect the slow movement of $Fe^{3+}O$ catalytic products through the subunit helices to the mineral growth cavity. Movement of $Fe^{3+}O$ multimers through the stable subunit α-helices in eukaryotic ferritins requires significant conformational change. Such changes will be slow in such a large protein assemblage (480 kDa). The contrast between the rates of active-site turnover (hours) and rapid catalytic coupling of two Fe and O atoms (microseconds) is enormous.

In 24-subunit ferritin protein cages, contrasting with the 12-subunit mini-ferritins, a nonbonded, four-α-helix polypeptide bundle forms around each 4-fold symmetry axis. The bundles form through the alignment of helix 5, extending from each of the four α-helix bundles. No function has been definitively established for the structure around the 4-fold symmetry axes, but deletion of helix 5 creates a protein cage that exposes the ferritin mineral to reductants and Fe^{2+} leakage.[25] The exits of the postoxidation channels, through which mineral nuclei travel between the active sites and the mineral growth cavity, are symmetrically placed around the 4-fold cage axes.[19]

3. FERRITIN FUNCTION

The ferritin function can be divided into two parts: (1) Fe^{2+} entry, catalytic redox with O_2, $Fe^{3+}O$ multimer formation (nucleation and mineral growth) and (2) mineral reduction/dissolution with Fe^{2+} exit/chelation. Each part occurs in different physical parts of the protein/mineral complex (channel transit, cage-based catalysis and nucleation, or the caged mineral surface) and in different time regimes—catalytic coupling of two Fe/O_2 (milliseconds) and nucleation/mineralization (minutes to hours). Because iron and dioxygen will react to form mineralized, hydrated ferric iron without the ferritin protein cage, the complexity of the ferritin function

must reflect the importance of rates and control over Fe^{2+} distribution.

Fe^{2+} entry into ferritin cages occurs spontaneously in solution but in vivo is likely dependent on transport by a protein "chaperone",[43] except during stress when normal regulatory/transport mechanisms are saturated. $Fe_2O_3{\cdot}H_2O$ mineral reduction and dissolution occur in response to physiological signals of iron need, in vivo, often referred to as the "size of the labile iron pool". In solution, the addition of a reductant triggers the mineral reduction and dissolution process, in which it is measured as the formation of Fe^{2+}-chelate complexes outside the protein cage (Figure 2). Ferritin functions are separated in space (within and inside the protein cage) and time (milliseconds to hours).

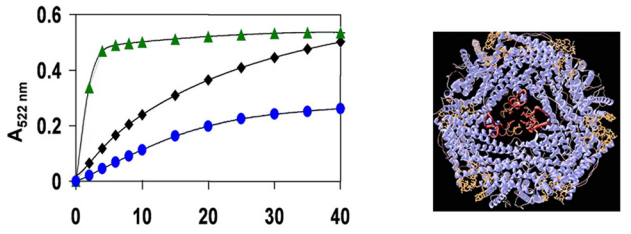

Figure 2. Protein control of ferritin mineral dissolution/Fe^{2+} chelation rates. Two heptapeptides selectively targeting the ferritin pore structure were isolated from a heptapetide library (10^9 peptides) and altered WT mineral dissolution and Fe^{2+} exit rates.[20] (Left) Fe^{2+} exit/chelation progress curves: green, peptide 1; blue, peptide 2; black, no peptide. (Right) Structures of the ferritin protein cage (blue), pore sequences, WT, folded (tan); L134P, unfolded (red). View: 3-fold symmetry axis centered. Ferritin mineral dissolution: NADH/FMN, reductant; Fe^{2+} bipyridyl, rate of Fe^{2+} exit. This research was originally published in *J. Biol. Chem.* **2007**, *282*, 31821.

a. Fe^{2+} Entry and Ion Channels. Fe^{2+} entry into ferritin protein cages is through the eight Fe^{2+} ion channels, at the 3-fold symmetry axes of 24-subunit ferritins. (There are four Fe^{2+} channels in the 12-subunit mini-ferritins.) The channels also influence Fe^{2+} exit after mineral reduction and dissolution.

Fe^{2+} entry through ferritin iron channels is currently measured through effects on the rates of enzymatic, Fe^{2+}/O redox reactions, which are also called "ferroxidase" or "F_{ox}" reactions. The reactions, which occur at diiron sites with some properties shared with diiron cofactor dioxygenases, cause spectral changes in the broad UV−vis absorbance range of 310−420 nm. However, it has not yet been possible to find distinct UV−vis spectral signatures that distinguish among all of the multiple ferric species, which include $Fe^{3+}O(H)Fe^{3+}$, the catalytic product/mineral precursor, mineral nuclei, and the mineral itself. Thus, the absorbance changes, in solutions of mineralizing ferritin protein cages, continue for many hours. In eukaryotic ferritins, Fe^{2+} entry and catalysis are monitored as the diferric peroxo [DFP_intermediate ($\lambda_{650\ nm}$)] that forms rapidly (milliseconds) from Fe^{2+}/O_2 and decays quickly (seconds; Figure 1C). DFP measurements allow determination of the effects of engineered amino acid variations in the Fe^{2+} entry ion channels and, elsewhere, on Fe^{2+}/O_2 reaction kinetics. Fe^{2+}/O redox reactions in ferritins are also studied by Mossbauer, resonance Raman, and X-ray absorption/extended X-ray absorption fine structure absorbance and electron paramagnetic resonance spectroscopies.[27,44−47] Direct binding of each Fe^{2+}, and the ligand structure, occurred at the diiron catalytic centers before O_2 binding in eukaryotic maxi-ferritins, indicated by VTVH magnetic circular dichroism (MCD)/circular dichroism (CD) analysis. By contrast, only a single Fe^{2+} binds at the catalytic centers of mini-ferritins, in the absence of O_2/H_2O_2.[38] Fe^{2+} entry through the ferritin ion channels has also been studied as s function of the Fe^{2+}/O_2 reaction or tryptophan fluorescence quenching.[12,48] Isothermal calorimetry, which is less specific, given the size of ferritin and the multiple channels and active sites, is also used to assess Fe^{2+}−ferritin protein interactions.[8] Intermediate stages in the movement of Fe^{3+} away from the catalytic sites to the mineral growth cavity in eukaryotic ferritins were studied for the first time, after site-specific residue assignments from combined solid-state and solution NMR, by comparison of $^{13}C-^{13}C$ NOESY ± Fe.[19]

b. Catalysis. Ferritin proteins catalyze the reaction between Fe^{2+} and O_2 (or H_2O_2 in Dps proteins). Each subunit has one diiron active site, with ligands from each of the four α-helices in each bundle; there is some variability in the iron ligands among different species and, in organisms with multiple tissues, among ferritins in different tissues (Table 1). In some 12-subunit Dps proteins, components of the active sites are donated by each of two subunits along the subunit dimer interfaces Table 1.[15] Catalysis is monitored using progress curves of $Fe^{3+}O$ formation (red line, Figure 1C), which has the disadvantage of spectral overlap between the early species, such as diferric peroxo and later species of diferric oxo/hydroxo and mineral. In animal ferritins, by contrast, the initial reaction intermediate, blue diferric peroxo, can be selectively measured[42,44−46] (Figure 1 C, blue line), using rapid mixing methods.

Ferritin diiron ligands at the catalytic sites have been examined by a variety of methods. Direct identification of Fe^{2+} ligands at the active sites in ferritin was achieved in a eukaryotic ferritin and a bacterial mini-ferritin (Dps protein), using VTVH MCD/CD.[10,38] For eukaryotic ferritins, the results confirm many of the inferences from the effects of deletional[49] and insertional mutagenesis[29] on solution kinetics, using nonspecific ($Fe^{3+}O$) and specific ($Fe^{3+}-O-O-Fe^{3+}$) spectral probes (Figure 1C), and from protein crystallography with proxy ions such as Zn^{2+}, Ca^{2+}, Mg^{2+}, and Co^{2+}.[28,30,33,50] Ferritin Fe^{3+}−ferritin protein crystals, obtained by soaking crystals with Fe^{2+} in air, showed differences from the Fe^{2+} sites in eukaryotic ferritins[51] likely representing the conformational differences between Fe^{2+} substrate and Fe^{3+} O product binding at the active sites.

Bacterial ferritin active sites, like those in eukaryotic ferritins, have been studied by crystallography and deletional mutagenesis for FTNA[35] and for the heme-containing BFR. Unlike diiron oxygenases, and BFR, where iron remains in the diiron site throughout catalysis, in eukaryotic ferritins iron is only transiently bound to the active site. Thus, in all crystallographic studies of eukaryotic ferritins, in contrast to the bacterial ferritin cofactor sites, proxy metals such as Co^{2+}, Cu^{2+}, or Zn^{2+} are observed in the active sites. Both bacterial ferritins, the heme and nonheme varieties, have an extra metal binding site C (Fe-3) that contributes to transfer of the catalytic products to the mineral growth cavity and to active-site regeneration. In archaeal ferritins, where there have been fewer opportunities for site direct mutagenesis combined with solution kinetic studies and where monitoring the catalytic intermediates appears to be complex, the ferritin active-site ligands are still changing.[27,36] While the understanding of ferritin catalytic mechanisms is more advanced in eukaryotic ferritins compared to the ferritins of bacterial adversaries in disease, much remains to be learned for all. Host/pathogen battles over iron involve

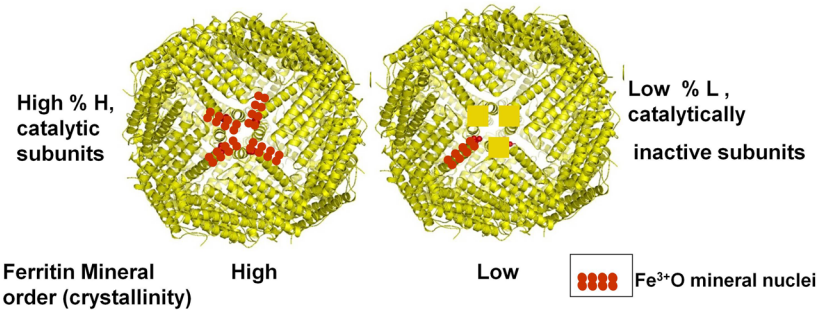

Figure 3. Differences mineral order among human tissue ferritins[6] coinciding with differences in the numbers of catalytic centers and nucleation channels/cage.[7] Ferritin protein cages rich in H subunits and with highly ordered ferritin minerals are found in tissues with high oxygenase, such as heart, while ferritin protein cages rich in L subunits and with relatively disordered minerals are found in human liver. The supply of stored iron to other tissues is a major function of liver ferritin, which is facilitated by the high surface/volume of the more disordered ferritin mineral.

host sequestration of iron in macrophage ferritin and the release of oxidants as antibacterial agents. Microbial virulence is associated with the production of mini-ferritins (Dps proteins[15,38,52,53]), with H_2O_2 as the oxidant. The differences between active-site structures, substrates (H_2O_2 vs O_2), and mechanisms in host and pathogen ferritins provide a tempting target for the development of antibacterial agents targeted at selective inhibition of bacterial mini-ferritin active sites.

c. Ferritin Mineral Nucleation. Ferritin minerals will nucleate at different places in the protein cage, which reflects the combination of ligands at the catalytic diiron sites, location of the catalytic sites, and number of active sites per cage. In 12-subunit mini-ferritins, the catalytic centers are most often on the inner surface of the mineral growth cavity,[15,39,54] suggesting that after oxidation and coupling the diiron products of catalysis are simply released into the mineral growth cavity. Differences in H:L subunit ratios in heart and liver coincide with differences in mineral order. Liver ferritin (H:L ∼ 1:4) has much more disordered mineral than heart ferritin (H:L ∼ 1:1).[6,55] An explanation is the number of $Fe^{3+}O$ nuclei that emerge near each other, around the 4-fold symmetry axes of the protein cage (Figure 3). On average, $Fe^{3+}O$ multimers in heart ferritin have a high probability of interacting with other $Fe^{3+}O$ multimers emerging from adjacent channels around the 4-fold symmetry axes to form large mineral nuclei and highly ordered minerals. By contrast, in liver ferritin (H:L ∼ 1:4), more solitary $Fe^{3+}O$ multimers will enter the mineral growth cavity, leading to less ordered mineral growth. Other than assessing the numbers of Fe atoms that can be accommodated in mini-ferritin cages, there has been little direct study of the mineral structure in mini-ferritins.

Among the 24-subunit mini-ferritins, the large number of carboxylate ligands on and near the interior surface of ferritins also led to hypotheses that mineral nucleation began at such carboxylates and mineral growth simply extended from such protein sites into the mineral growth cavity. Such conjectures were supported by the inhibition of mineral formation caused by replacement of surface carboxylates on mineral nucleation in catalytically inactive L ferritins lacking cavity surface carboxylates E55, E60, and E63.[56,57] (Residue numbers are the classical ferritin sequence that applies to all eukaryotic subunits; for human H ferritin numbering, add 4.) In ferritins without catalytic sites, Fe^{2+} can enter the ferritin protein cage through the eight ion channels at the 3-fold symmetry axes, exit directly into the mineral growth cavity, and be oxidized by dioxygen dissolved in the cavity fluid because there is no competition for Fe^{2+} by the diiron centers. However, when catalytic centers are present (H ferritin), replacement of nucleation center residues (E60 and E63) had no effect on catalysis or mineral growth,[58] presaging the identification of the nucleation channels.[19]

The Fe^{3+} O nucleation channels (Figures 1B and 3) in eukaryotic ferritins, as identified by the paramagnetic effects of Fe^{3+} on $^{13}C-^{13}C$ NOESY spectra, at ∼50 Å are longer than the Fe^{2+} ion entry channels and pass through the center of the four α-helix bundles of each subunit to connect catalytic centers and mineral growth cavity in eukaryotic ferritins. Movement of the $Fe^{3+}O$ multimers will be slowed by the rigidity of the four α-helix bundles, which likely explains the long periods of time required for turnover of the catalytic sites.[41,42] Covariation between active-site and nucleation-channel amino acids[4] emphasizes the interdependence between catalysis and transfer of the $Fe^{3+}O$ products to the mineral growth cavity of eukaryotic ferritins.[4] Coupled with the contributions of ion-channel residues to catalysis that are[4,12] integrated function throughout each ferritin subunit, over 50 Å, becomes clear. Still to be understood are the persistent observations of protein−protein cooperatively related to cage self-assembly and function.[8,10] Ferritin nucleation channels, and their relationship to the presence of ferritin catalytic sites and minerals with different crystalline order[6] (Figure 3), can be exploited to control product structures when ferritin protein cages are used as nanovessels and nanotemplates for drug delivery and nanosensors.[8,59−63]

The later stages in ferritin iron mineralization remain poorly understand in part because of the lack of easily accessible spectroscopic markers that resolve the products of catalysis into one more intermediate. Mössbauer analysis of multimeric $Fe^{3+}O$ intermediates in mineralization becomes very complex beyond iron dimers.[64] The effects of replacing key amino acids on the ferritin $Fe^{3+}O$ spectrum (A = 310−42 nm)[31] suggest that such goals may be accessible. Experimental study of ferritin protein cages composed of defined mixtures of heterogeneous subunits, either natural[17] or chemically produced,[8] is key to full understanding Nature's array of tissue-specific differences in ferritin protein cages and minerals.

d. Reduction/Dissolution of Ferritin Protein-Caged Mineral. Sometimes called "iron release" or "Fe^{2+} exit", the reduction and dissolution of a caged ferritin mineral is studied by adding a reductant to solutions of ferritin (caged mineral + protein) and trapping mineral reduced and dissolved as an Fe^{2+}-chelator complex. In solution, the reductants most often used are $[S_2O_4]^{2-}$ or the biological mixture of NADH and FMN. Dithiothreitol is also used, even though it is slow, because dithionite can modify the proteins.[65] Some the

dx.doi.org/10.1021/ic400484n | Inorg. Chem. 2013, 52, 12223−12233

reductants appear to enter the protein cage,[65] and, thus, Fe^{2+} exits after mineral dissolution and iron chelation rates are controlled by the dynamics of opening and closing the protein cage pores, as well as by the surface effects of mineral dissolution; see Figure 2.[20,23] When iron chelator complexes are colored, the measurement of ferritin iron mineral dissolution of the iron derivative is color-facilitated; filtration studies show that Fe^{2+}-chelates (bipyridyl) are outside the protein cage.[66] The Fe^{2+}-bipyridyl complex is measured by UV−vis spectrometry. If Fe^{3+} chelators are used, the kinetics of Fe^{2+} removal from ferritin minerals is complicated by the oxidation to Fe^{3+}.

The ferritin function is sometimes studied in cultured living cells rather than in solution. The cells grow on a complex medium, e.g., Dulbecco's modified Eagle's Medium (DMEM), which is a neutral solution containing vitamins, amino acids, glucose, phosphate, and other salts; DMEM is usually mixed with 10% serum. Thus, only 10% of the normal transferrin is present and, unless extra iron is added, only 10% of the environmental iron normal for mammalian cells. Cultured mammalian cells are usually incubated in an atmosphere of 5% CO_2 in air, which at 20% O_2 is much more concentrated than oxygen dissolved in blood (~5% O_2); dissolved CO_2 provides a HCO_3^{-1} buffer and the synergistic anion for transferrin−Fe binding. In some studies,[59] Fe-transferrin was used to examine ferritin iron turnover/chelator binding,[24] while in the peptide uptake studies described here, cells were incubated with or without ^{125}I-tyrosine-labeled peptide; labeling used solid-phase 1,3,4,6-tetrachloro-3a,6a-diphenylglycoluril (Thermo Pierce) reagents with a peptide previously identified as unfolding surface pores in ferritin protein pores.[20] Recovered cells were washed with buffer-containing unlabeled peptide to measure the specifically bound peptide in whole cells and in cellular proteins precipitated with 5% trichloroacetic acid.

Changes in the cellular amounts of ferritin protein, which are increased by iron (mRNA target)[67,68] or heme and oxidative stress (DNA target)[69,70] or both, are measured using immunological reactions (immunoprecipitation or immunoblots, often called, "Western blots"). The intracellular distribution of mineralized ferritin is assessed by microscopy of the mineral itself. For exogenous ferritin proteins, fluorescent labels can be coupled with electron microscopy. The key to opening iron-chelation therapies equally to heart and liver ferritin iron, in humans at risk for lethal iron accumulation in Thalassemia and Sickle Cell Disease,[16,71] may well be understanding the tissue specificity of ferritin protein cage control over ferritin mineral order, crystallinity, and chelator access.

4. FERRITIN MINERAL

a. Mineral Structure. X-ray diffraction, X-ray absorption, electron microscopy (scanning transmission electron microscopy, transmission electron microscopy, etc.), and density (usually sedimentation/ultracentrifugation, often through sucrose gradients) are all used to examine ferritin minerals. The low phosphate form of ferritin minerals that are found in animals is hydrated ferric oxide/hydrous ferric oxyhydroxide and is most similar to ferrihydrite, a nanomineral: $5Fe_2O_3 \cdot 9H_2O$. Such minerals have 20% tetrahedrally and 80% octahedrally coordinated Fe^{3+}. Ferritin minerals vary in size, limited by both the wall of the spherical central cavity (5 or 8 nm diameter) and the availability of Fe^{2+} and the oxidant. The use of techniques provided single-molecule information on ferritins more than half a century before the single-molecule experiments of contemporary science.

b. Mineral Function. Monitoring the fate of ^{59}Fe or ^{55}Fe-radiolabeled ferritin in different tissues is a common method for studying the function of ferritin minerals. Whole body, tissue, or cell radioactivity is measured in samples of tissue; measuring red blood cell ^{59}Fe or ^{55}Fe radioactivity is another common technique used. In situations where a tissue biopsy is performed for other purposes, radiolabeled iron in the tissue samples can also be analyzed. Such studies have been used to study the absorption of iron from different sources[72−75] and the redistribution in a legume of nodule iron (nitrogenase and leghemoglobin) to seeds (ferritin mineral).[76]

Isotope experiments have the requirement that the "reporter" isotope or "tracer" must equilibrate with the material being traced. An example of the difficulties that occur when this condition is not met is experiments about the bioavailability of iron in beans. Experiments carried out 30 years, where the tracer did not equilibrate with bean ferritin iron, reached the conclusion that bean iron was not bioavailable. In the experiment, $^{59}FeCl_3$ was added to ground beans before consumption. $^{59}FeCl_3$ did not equilibrate with the ferritin mineral iron and even worse was chelated by a normal bean component, phytic acid, which is poorly absorbed.[77] The conclusion was reached that anemia, prevalent in many populations (30% worldwide), would not be cured by increasing the consumption of iron-rich beans.[77] Approximately 10 years later, the experiments were repeated in beans from plants cultivated with ^{59}Fe-EDTA (EDTA = ethylenediaminetetraacetic acid) during growth and seed formation. In these experiments, equilibration of the label with the iron in bean ferritin mineral was possible, and the results showed clearly that bean iron is bioavailable both in model animal studies and in humans.[78,79] However, even today the issue is still being examined experimentally.[80]

c. Mineral Dissolution and Fe^{2+} Exit. How iron is recovered from the ferritin mineral in vivo has been little studied. However, iron-chelation therapies in human disease would be facilitated by such information. Often, in the study of ferritin, extra iron was added to increase the amount of ferritin protein and facilitate ferritin detection. However, apparently the added iron was high enough to be toxic, and cells responded by engulfing the extra ferritin in an intracellular compartment, the lysosome. The observation was interpreted to mean that the normal pathway for recovering iron from ferritin was destruction by lysosomal enzymes. If this were so, there would be no evolutionary advantage to the complex genetic regulatory system that controls ferritin biosynthesis. Moreover, enormous amounts of cell energy would be consumed (1 GTP for each of the >4000 peptide bonds) in the synthesis of a protein, where the only function is to be degraded with the generation of exposed, reactive iron mineral! Ferritin protein is degraded, in a regulated manner, i.e., only when the cell is iron-deficient and the ferritin iron content is low.[81,82] The ferritin protein degradation site is the proteasome in the cell cytoplasm.[83] The degradation signal for low iron ferritin is not known, but after multiple cycles of electron transfers in the Fe^{2+}/O_2 catalytic reaction and $Fe_2O_3 \cdot H_2O$ synthesis, peptide bond breakage or amino acid side-chain oxidation may reach a level sensed as "excessive". Ferritin iron can be recovered by adding external reductants and chelators in solution or injection/absorption chelators in vivo, but the process is slow

because most of the time ferritin protein cages block reductant access to ferritin mineral.

Ferritin protein cages are very stable, resisting 6 M urea at pH 7 or >80 °C, pH 7, in solution. Nevertheless, regions of local instability in the protein cage unfold at 56 °C or 1 mM urea.[23] They are at the external pores of the ion channels in ferritin protein cages and essentially "open" the ferritin cage pores. Opening/unfolding the pores increases the rates of ferritin mineral dissolution (Fe^{2+} exit). Many of the pore residues are highly conserved; substitution of channel residues also "opens" the pores. Recently, when the ferritin dimer interface was modified so single, folded ferritin subunits could be produced and studied, the subunits unfolded 40 °C below that of the cage, T_m = 80 °C,[8] showing the enormous stabilization conferred on the protein cage by intersubunit interactions. In cultured human cells, when ferritin pore unfolding was increased by mutation, iron retention by the altered ferritin was significantly lower than that in wild type (WT) protein under the same conditions.[24]

During iron toxic states created by modern transfusion therapies, which bypass the homeostatic control mechanisms for iron absorption in the intestine, increased ferritin protein synthesis cannot keep up with the increased iron entering the body. As a result, the iron content of each ferritin protein increases above normal (3−4000 Fe atoms/protein cage compared to ∼2000 Fe atoms/protein cage). Eventually, the ferritin protein cages are damaged, which exposes ferritin iron mineral to cytoplasmic reductants and initiates redox chemistry involving free radicals and protein damage. Damaged ferritin is called hemosiderin, which is functionally defined as insoluble cellular iron. (Native ferritin is very soluble, >100 mg/mL.) The cell response to ferritin protein cage damage and hemosiderin formation is autophagy, explaining iron mineral accumulation into lysosomes of cells grown with high concentrations of iron; the result is to deprive the cell cytoplasm of the antioxidant effect of ferritin protein.

5. REGULATED FERRITIN PROTEIN BIOSYNTHESIS (ROLE OF THE MRNA STRUCTURE AND PROTEIN BINDING)

In health, ferritins supply metabolic iron concentrates for cellular syntheses of iron proteins in the cytoplasm and mitochondria, making them particularly important preceding mitochondrial division and cell growth. The ability of ferritins to scavenge free iron and to consume dioxygen makes them effective response proteins after normal or pathological oxidative damage.

a. Ferritin mRNA Biosynthesis−Transcriptional Control. The transcriptional regulation of ferritin genes is coordinated with a large group of proteins that are important in restoring the cytoplasm of a cell to normalcy after oxidant stress (thioredoxin reductase, heme oxygenase, NADPH-quinone reductase, etc). The genes are regulated, in part, through interactions of the ARE (antioxidant response element) promoter and Bach1 repressor protein, a DNA binding protein that binds the ARE DNA sequence until heme binds to Bach 1; each ARE has different binding affinities for Bach 1,[70] which allows a set of quantitatively different responses among the genes for each biological signal. These proteins all contribute to the reestablishment of normal redox in cells. The consumption of Fenton chemistry reactants, Fe^{2+} and O_2 in making protein-caged biominerals, makes ferritin an antioxidant, illustrating its ARE gene regulation.

b. Ferritin Protein Cage Biosynthesis−Translational Control. Ferritin biosynthesis has been most studied in animals. When cellular iron concentrations are low, ferritin mRNA is stored in the cytoplasm as a complex with IRP1 or IRP2 bound to the IRE-RNA, noncoding riboregulator. When cellular iron concentrations are high, IRE1 or IRP2, Fe^{2+} binds to the IRE and changes the RNA conformation, which causes IRP dissociation to increase.[2,3] As a result, IRP dissociates from the IRE-RNA, eIF4F binds, and ferritin mRNA translation increases.[2,3] Ferritin protein subunits are always found in assembled cages.

c. Ferritin Protein Cage/Fe^{2+}/O Feedback Loop. Regulated ferritin protein biosynthesis is unusual because DNA (transcription) and mRNA (translation are regulated) and the regulatory signals are both inorganic and organic [heme, Fe^{2+}, and oxidants (O)] and are related to the substrates used by the encoded protein (ferritin cages), Fe^{2+} and O_2 or H_2O_2. When heme binds to Bach1, transcription of ferritin genes/ferritin mRNA biosynthesis increases. When cells have oxidant damage or large excesses of iron ferritin, gene transcription also increases. As a result, Fe and O (O_2, H_2O_2, and "oxidant") are part of a feedback loop involving DNA, mRNA, and the gene product (ferritin protein cages) that consume Fe^{2+} and O_2 to synthesize the caged ferritin mineral, $Fe_2O_3{\cdot}H_2O$. Fe^{2+} and O_2 or oxidant are genetic "signals" and, for Fe^{2+} and O_2, protein substrates. Three protein regulators in the feedback loop are known to date: Bach 1, a DNA or heme binding transcriptional repressor IRPs (two mRNA binding translation repressor proteins), and eIF-4F, an RNA binding translational enhancer that facilitates ribosome binding to mRNA.[3,70]

Excess Fe or O activate ferritin DNA and mRNA to synthesize more ferritin protein. Diiron catalytic sites in ferritin protein cages consume the Fe and O substrates that are also the genetic signals, shutting down ferritin gene transcription and ferritin mRNA translation/protein synthesis.[84] When plants, animals, or people are iron-deficient, ferritin synthesis is diminished, but in plants, ferritin iron-dependent ferritin regulation is restricted to mRNA synthesis.[85] The critical nature of ferritin to animal life is emphasized by the unique metabolite signal/gene/protein substrate feedback loop and by the embryonic lethality of gene deletions in mice.[86] Heme iron is the signal for DNA regulation by the Bach1 transcription regulatory protein,[70] while Fe^{2+} binding to an mRNA regulator (IRE) is the signal for DNA-independent regulation of protein biosynthesis.[2,3]

6. FERRITIN AS A THERAPEUTIC TARGET AND DELIVERY AGENT IN DISEASE

Iron−ferritin interactions contribute to several disease responses. First, ferritins decrease iron available to pathogens by decreasing serum iron that normally is derived from the recycling of old red blood cells. The result is "the anemia of chronic disease".[67] Second, when hosts release damaging oxidants, successful pathogens synthesize mini-ferritins (u proteins). Dps proteins are mini-ferritins (12-subunit protein cages) that use H_2O_2 to make ferritin mineral, thereby resisting the antibacterial H_2O_2 released by the host. Finally, when tissue damage in disease is extensive, as in the lungs in cystic fibrosis, ferritin escaping from damaged cells is absorbed by opportunistic pathogens.[87] Targets in ferritin protein cages for pharmacological exploitation are the selective properties of mini-ferritin (Dps protein) active sites, pores around the 3-fold

axes of the protein cages, the ferritin IRE-mRNA riboregulator, and the dimer interface of the subnit helix bundle, where geometric interdigitation of the amino acid side chains controls cage assembly.

a. Selective Properties of Mini-Ferritin (Dps Protein) Catalytic Sites as a Target for Selective Inhibition of Catalysis. The development of selective small-molecule inhibitors is a basic component of drug design. The active sites in 12-subunit mini-ferritin (Dps protein) differ in structure (number of ligands, location in the protein cage, etc.; Table 1), oxidant (H_2O_2 vs O_2), and order of addition of the two substrates (binding of the second Fe^{2+} requires oxidant binding).[15,20,26] Currently, mini-ferritins of human pathogens have been targeted as antigens in vaccines. However, the idea of weakening bacteria during infection by inhibiting the catalytic functions of their mini-ferritins has been little considered, even though the active protein is associated with bacterial virulence.

b. Ferritin Protein Cages as Targets for Chelators in Transfusional Iron Overload during the Treatment of Genetic Anemias. Ferritin is the site of most of the excess iron in the genetic diseases of iron overload. In hereditary hemochromatosis, excess iron accumulates because of a genetic defect in a protein, HFE, which interferes with the normal signaling of adequate iron absoprtion. In the genetic anemias, Thalassemia and Sickle Cell Disease, the treatment itself, transfusion of normal red blood cells, causes iron overload. A major physiological response to excess iron is increased ferritin protein biosynthesis mainly through the effects of Fe^{2+}−IRE-RNA binding on interactions with regulatory protein binding (IRP or eIF-4F) described in part 4. Under the best of conditions, however, the amounts of protein synthesized are too small for the amounts of accumulated iron and, during iron overload, the average size of the iron mineral in the ferritin protein cage increases.[88,89] The homeostatic responses that have evolved are clearly overwhelmed by contemporary medical therapies.

In hereditary hemochromatosis, excess iron is removed by regular phlebotomy and the blood is used by blood banks,[90] because iron excretion is very low in mammals.[67] However, excess iron from hypertransfusions in genetic anemia cannot be removed by phlebotomy because the genetic defects are in red cell production.

To remove excess iron in hypertransfusion iron overload, a variety of iron chelators have been developed over the last 40 years. Some chelators are from bacterial siderophore models. The three iron chelators in common use today are deferral, desferriox, and deferiprone.[91] Combinations of iron chelators are particularly effective[92] in part because of differences in the subcellular location of the different chelators.[93] The iron chelator desferrioxamine (Desferal) folds without iron and, thus, enters cells by endocytosis into the lysosomal compartment. By contrast, deferriprone and desferasirox require iron to fold, and the linear molecules enter cells by transport through the plasma membrane. Desferal is administered intravenously, and deferriprone and desferasirox are administered orally. The major problem with current iron chelators is that they target low molecular iron (the "labile iron pool"),[16,71] which is only a small fraction of excess iron. Most of the excess iron in the solid protein coated the ferritin mineral. The rationale used for such chelators is that all the iron in living cells, including iron in the ferritin mineral is in equilibrium. As a result, current chelation regimens are very slow and long, sometimes as long as 40 h/week. The idea of targeting chelators to ferritin protein pores, using specific binding partners, e.g., peptide (see Figure 2), that readily enters cells (HepG2cell cultures; Theil, E. C.; Wang, H., unpublished observations) remains underdeveloped.

c. Ferritin mRNA Riboregulators as Small-Molecule Targets To Increase Ferritin Protein Synthesis and Minimize Toxic Hemosiderin (Damaged Ferritin). The compensatory responses to iron overload are incompletely matched. For example, even though ferritin protein biosynthesis increases to manage the cellular iron, the iron content of each ferritin protein cage increases.[25] Denatured ferritin (toxic hemosiderin) also increases. Little iron is excreted in the urine during iron overload because, unlike other metal ions, ion excretion is minimal, even when the tissue iron content is abnormally high.

Increasing the ferritin protein synthesis with small molecules targeting the ferritin mRNA riboregulator will decrease the iron content of ferritin protein cages and of hemosiderin during iron overload. Synthesizing more ferritin protein during iron overload will decrease ferritin cages that are by mineralization of excess caged iron. Moreover, additional sites for safe iron storage will be produced. Three observations support the rationale: First, the ferritin riboregulator (IRE-RNA) selectively binds small molecules and two regulatory proteins, one of which blocks ribosome binding to mRNA and the other of which enhances ribosome binding to mRNAs;[3,68] conformational change in IRE-RNA induced by RNA-Fe^{2+} binding[3] is the trigger that decreases IRP binding and increases eIF-4F binding. The result is a change in the ferritin protein biosynthesis rates in vitro whether IRE-RNA is changed by binding a small, organic molecule[94] or by binding Fe^{2+3}. Second, during iron overload, a significant fraction of ferritin mRNA molecules remain repressed in vivo.[95] Third, increasing the ferritin protein concentration by activating the pool of ferritin mRNA still blocked during iron overload[95] is benign to human physiology: overproduction of ferritin subunits and assembled cages, caused by mutations in the IRE riboregulator (hereditary hyperferrtinemia cataract syndrome), for example, has only minor effects on human physiology.[96]

d. Ferritin Protein Cages as Nanovessels for Drug or Sensor Delivery. Ferritin protein cages are emerging as novel components of disease therapies.[97] The use of human ferritin protein cages has the added benefit of minimizing immune reactions. Intact ferritin enters living cells by receptor-mediated endocytosis.[98,99] Ferritin protein cages have been used to deliver sensors of uniform sizes for imaging,[100,101] for detection of vascular inflammation and angiogenesis in carotid and aortic disease,[62] and as compounds that are potential antitumor agents. A potential limit in using ferritin to deliver drugs or agents is fitting the desired cargo inside the cage. In some natural ferritins, cross-links between pairs of subunits along the 2-fold symmetry axes of the protein cage change the size of the caged ferritin mineral.[81] Recently, an engineered ferritin cage was produced with changed interactions along the cage dimer interface so that cage disassembly/assembly was controlled with Cu^{2+}.[8] The modified ferritin protein cage was disassembled and reassembled around a large molecular cargo. Such an approach allows large molecules close to the size of the ferritin mineral cavity to be captured inside ferritin. How cells will react to such complexes remains to be explored. However, when an animal cell absorbs a foreign (plant) ferritin by endocytosis, the plant ferritin protein cage is degraded and the iron mineral content is made available to the cell for metabolism.[98,102] With such observations in hand to place desired compounds inside the

dx.doi.org/10.1021/ic400484n | Inorg. Chem. 2013, 52, 12223−12233

ferritin cages and modifications of ferritin surfaces for selective delivery, the ability to deliver concentrated doses of drugs to particular cell types is imminent.

7. PERSPECTIVE

Ferritin protein chemistry protects cells from Fenton chemistry substrates Fe^{2+}, O_2, or H_2O_2, which are released from their normal locations by oxidative damage. Ferritin converts Fe^{2+} and O_2 to the caged Fe/O mineral. The mineral also preserves the iron in a concentrated from for use in the cofactor synthesis during cell recovery. Fe^{2+} binding to ferritin ion entry/exit channels and protein catalytic sites, as well as the binding of $Fe^{3+}O(H)$ multimeric products near active sites in protein nucleation channels and around the 4-fold symmetry axes inside the cage, are only partly understood; they also appear to depend on which member of the ferritin superfamily is being studied. Variations in the ferritin amino acid sequence (up to 80%), active-site ligands, location of the active sites (Table 1), protein cage size (12 or 24 subunit cages), and numbers of catalytically active subunits/cage (4−24) and interrelated variations in the protein mineral crystallinity (Figure 3) indicate that Nature has already matched ferritin structures to multiple physiological and environmental conditions. As long as chemists avoid the trap of blurring the variations with overly rigid reductionism, the natural, biological variety among ferritin proteins provides a rich platform to develop a ferritin nanocage for many technical and medical needs.

The amount of iron needed for health is well-defined. In humans who are not growing or reproducing, only 1−2 mg/day absorbed is needed to maintain normal health. (Absorption from food iron is ∼10−20% efficient among all of the different chemical forms of iron in food, so ∼10−20 mg/day needs to be eaten.) Nevertheless, iron deficiency is the major nutritional deficiency in the world today, ∼500 years after the original diagnoses and development of treatments.[103] Successful organisms are programmed to synthesize ferritin in times of "plenty", in anticipation of future use. Thus, ferritin is most abundant in stationery cultures of bacteria awaiting triggers for rapid growth,[5,104] in legume nodules preparing for nitrogen fixation,[104] where nitrogenases (32 Fe/protein) and leghemoglobin are synthesized in abundance, in immature leaves preparing for photosynthesis and ferredoxin synthesis,[105] in embryonic erythrocytes before the rapid cell replacement associated with hemoglobin "switching",[106] and in fetal liver[107] in anticipation of the developmental, neonatal iron deficit. Ferritin iron mineral dissolution occurs when cellular demands inside the organisms change, such as cell division or rapid growth (childhood, puberty). The signals that regulate cellular developmental programs to "plan ahead" for iron use are still obscure, although a recent study indicates a study role for the heme binding proteins Bach1 as a mitosis regulator.[108]

Gaps in the chemical and molecular biological information about normal iron homeostasis and normal development negatively impact the understanding of the medical problems associated with massive iron accumulations above normal homeostatic mechanisms. Toxic iron accumulations occur as a result of hypertransfusion treatment in hereditary hemoglobin defects (Thalassemia and Sickle Cell Disease), transfusions after chemotherapy or before transplants (e.g., CNS tumors, leukemia, sarcomas, lymphomas, and renal carcinomas), and excess iron absorption from food in hereditary hemochromatosis. Ferritin and hemosiderin (damaged ferritin) are the major sites of the abnormal iron deposits in humans. Small-molecule iron chelators can access only a small fraction of the iron needed to be removed because solid ferritin minerals are protected from the chelators and cellular reductants by the folded protein cage. New strategies such as binding peptides, which modulate folding of ferritin proteins pores,[20,23] to increase chelation are in very early stages and require extensive "translation" and development before they are ready for removal of iron from humans with toxic iron overload. Other uses of ferritins being developed for use in disease are as nanovessels for drug delivery and templates for sensors.[61,62,107] Finally, ferritin mRNA riboregulators are both models for mRNA exploitation in general and potential aids during iron excess, in particular. During the billions of years that ferritins have existed, differences in the protein cages have evolved to match particular environmental niches (aerobic, anaerobic, single cells, multiple cells, and tissues) and for different physiological purposes (DNA protection, recovery from oxidant stress, providing metabolic iron concentrates, and sequestering iron from invading pathogens). The attractive, natural array of ferritin variants requires further exploration for a full understanding and novel applications to human health and disease.

AUTHOR INFORMATION

Corresponding Author

*E-mail: etheil@chori.org. Tel: 510-450-7670. Fax: 510-597-7131.

Notes

The authors declare no competing financial interest.

ACKNOWLEDGMENTS

The author thanks all of her group members and colleagues for their enthusiastic intellectual and technical contributions to the work described here. Support from the NIH (Grant R01-DK20251), the CHORI Foundation, and CHORI Partners has been crucial.

REFERENCES

(1) Hsiao, C.; Chou, I. C.; Okafor, C. D.; Bowman, J. C.; O'Neill, E. B.; Athavale, S. S.; Petrov, A. S.; Hud, N. V.; Wartell, R. M.; Harvey, S. C.; Williams, L. D. *Nat. Chem.* **2013**, *5*, 525−528.

(2) Khan, M. A.; Walden, W. E.; Goss, D. J.; Theil, E. C. *J. Biol. Chem.* **2009**, *284*, 30122−30128.

(3) Ma, J.; Haldar, S.; Khan, M. A.; Sharma, S. D.; Merrick, W. C.; Theil, E. C.; Goss, D. J. *Proc. Natl. Acad. Sci. U. S. A.* **2012**, *109*, 8417−8422.

(4) Haldar, S.; Bevers, L. E.; Tosha, T.; Theil, E. C. *J. Biol. Chem.* **2011**, *286*, 25620−25627.

(5) Nandal, A.; Huggins, C. C.; Woodhall, M. R.; McHugh, J.; Rodriguez-Quinones, F.; Quail, M. A.; Guest, J. R.; Andrews, S. C. *Mol. Microbiol.* **2010**, *75*, 637−657.

(6) St. Pierre, T.; Tran, K. C.; Webb, J.; Macey, D. J.; Heywood, B. R.; Sparks, N. H.; Wade, V. J.; Mann, S.; Pootrakul, P. *Biol. Met.* **1991**, *4*, 162−165.

(7) Theil, E. C. *Curr. Opin. Chem. Biol.* **2011**, *15*, 304−311.

(8) Huard, D. J.; Kane, K. M.; Tezcan, F. A. *Nat. Chem. Biol.* **2013**.

(9) Fletcher, J. M.; Harniman, R. L.; Barnes, F. R.; Boyle, A. L.; Collins, A.; Mantell, J.; Sharp, T. H.; Antognozzi, M.; Booth, P. J.; Linden, N.; Miles, M. J.; Sessions, R. B.; Verkade, P.; Woolfson, D. N. *Science* **2013**, *340*, 595−599.

(10) Schwartz, J. K.; Liu, X. S.; Tosha, T.; Theil, E. C.; Solomon, E. I. *J. Am. Chem. Soc.* **2008**, *130*, 9441−9450.

(11) Tosha, T.; Behera, R. K.; Ng, H.-L.; Bhattasali, O.; Alber, T.; Theil, E. C. *J. Biol. Chem.* **2012**, *287*, 13016−13025.

(12) Tosha, T.; Behera, R. K.; Theil, E. C. *Inorg. Chem.* **2012**, *51*, 11406−11411.
(13) Ragland, M.; Briat, J. F.; Gagnon, J.; Laulhere, J. P.; Massenet, O.; Theil, E. C. *J. Biol. Chem.* **1990**, *265*, 18339−18344.
(14) Grant, R. A.; Filman, D. J.; Finkel, S. E.; Kolter, R.; Hogle, J. M. *Nat. Struct. Biol.* **1998**, *5*, 294−303.
(15) Chiancone, E.; Ceci, P. *Biochim. Biophys. Acta* **2010**, *1800*, 798−805.
(16) Lal, A.; Porter, J.; Sweeters, N.; Ng, V.; Evans, P.; Neumayr, L.; Kurio, G.; Harmatz, P.; Vichinsky, E. *Blood Cells Mol. Dis.* **2013**, *50*, 99−104.
(17) Rucker, P.; Torti, F. M.; Torti, S. V. *Protein Eng.* **1997**, *10*, 967−73.
(18) Matzapetakis, M.; Turano, P.; Theil, E. C.; Bertini, I. *J. Biomol. NMR* **2007**, *38*, 237−242.
(19) Turano, P.; Lalli, D.; Felli, I. C.; Theil, E. C.; Bertini, I. *Proc. Natl. Acad. Sci. U. S. A.* **2010**, *107*, 545−550.
(20) Liu, X. S.; Patterson, L. D.; Miller, M. J.; Theil, E. C. *J. Biol. Chem.* **2007**, *282*, 31821−31825.
(21) Li, C.; Pielak, G. J. *J. Am. Chem. Soc.* **2009**, *131*, 1368−1369.
(22) Bermel, W.; Bertini, I.; Felli, I. C.; Matzapetakis, M.; Pierattelli, R.; Theil, E. C.; Turano, P. *J. Magn. Reson.* **2007**, *188*, 301−310.
(23) Liu, X.; Jin, W.; Theil, E. C. *Proc. Natl. Acad. Sci. U. S. A.* **2003**, *100*, 3653−3658.
(24) Hasan, M. R.; Tosha, T.; Theil, E. C. *J. Biol. Chem.* **2008**, *283*, 31394−31400.
(25) Arosio, P.; Levi, S. *Biochim. Biophys. Acta* **2010**, *1800*, 783−792.
(26) Le Brun, N. E.; Crow, A.; Murphy, M. E.; Mauk, A. G.; Moore, G. R. *Biochim. Biophys. Acta* **2010**.
(27) Honarmand Ebrahimi, K.; Bill, E.; Hagedoorn, P. L.; Hagen, W. R. *Nat. Chem. Biol.* **2012**, *8*, 941−948.
(28) Hempstead, P. D.; Yewdall, S. J.; Fernie, A. R.; Lawson, D. M.; Artymiuk, P. J.; Rice, D. W.; Ford, G. C.; Harrison, P. M. *J. Mol. Biol.* **1997**, *268*, 424−448.
(29) Liu, X.; Theil, E. C. *Proc. Natl. Acad. Sci. U. S. A.* **2004**, *101*, 8557−8562.
(30) Toussaint, L.; Bertrand, L.; Hue, L.; Crichton, R. R.; Declercq, J. P. *J. Mol. Biol.* **2007**, *365*, 440−452.
(31) Tosha, T.; Hasan, M. R.; Theil, E. C. *Proc. Natl. Acad. Sci. U. S. A.* **2008**, *105*, 18182−18187.
(32) Masuda, T.; Goto, F.; Yoshihara, T.; Mikami, B. *J. Biol. Chem.* **2009**.
(33) Tosha, T.; Ng, H. L.; Bhattasali, O.; Alber, T.; Theil, E. C. *J. Am. Chem. Soc.* **2010**, *132*, 14562−14569.
(34) Stillman, T. J.; Connolly, P. P.; Latimer, C. L.; Morland, A. F.; Quail, M. A.; Andrews, S. C.; Treffry, A.; Guest, J. R.; Artymiuk, P. J.; Harrison, P. M. *J. Biol. Chem.* **2003**, *278*, 26275−26286.
(35) Crow, A.; Lawson, T. L.; Lewin, A.; Moore, G. R.; Le Brun, N. E. *J. Am. Chem. Soc.* **2009**, *131*, 6808−6813.
(36) Tatur, J.; Hagen, W. R.; Matias, P. M. *J. Biol. Inorg. Chem.* **2007**, *12*, 615−630.
(37) Liu, X.; Kim, K.; Leighton, T.; Theil, E. C. *J. Biol. Chem.* **2006**, *28*, 27827−27835.
(38) Schwartz, J. K.; Liu, X. S.; Tosha, T.; Diebold, A.; Theil, E. C.; Solomon, E. I. *Biochemistry* **2010**, *49*, 10516−10525.
(39) Papinutto, E.; Dundon, W. G.; Pitulis, N.; Battistutta, R.; Montecucco, C.; Zanotti, G. *J. Biol. Chem.* **2002**, *277*, 15093−15098.
(40) Li, M.; Yun, S.; Yang, X.; Zhao, G. *Biochim. Biophys. Acta* **2013**.
(41) Waldo, G. S.; Theil, E. C. *Biochemistry* **1993**, *32*, 13262−13269.
(42) Treffry, A.; Zhao, Z.; Quail, M. A.; Guest, J. R.; Harrison, P. M. *Biochemistry* **1997**, *36*, 432−441.
(43) Leidgens, S.; Bullough, K. Z.; Shi, H.; Li, F.; Shakoury-Elizeh, M.; Yabe, T.; Subramanian, P.; Hsu, E.; Natarajan, N.; Nandal, A.; Stemmler, T. L.; Philpott, C. C. *J. Biol. Chem.* **2013**, *288*, 17791−17802.
(44) Pereira, A. S.; Small, W.; Krebs, C.; Tavares, P.; Edmondson, D. E.; Theil, E. C.; Huynh, B. H. *Biochemistry* **1998**, *37*, 9871−9876.
(45) Moenne-Loccoz, P.; Krebs, C.; Herlihy, K.; Edmondson, D. E.; Theil, E. C.; Huynh, B. H.; Loehr, T. M. *Biochemistry* **1999**, *38*, 5290−5295.
(46) Hwang, J.; Krebs, C.; Huynh, B. H.; Edmondson, D. E.; Theil, E. C.; Penner-Hahn, J. E. *Science* **2000**, *287*, 122−125.
(47) Zhao, G.; Arosio, P.; Chasteen, N. D. *Biochemistry* **2006**, *45*, 3429−3436.
(48) Bellapadrona, G.; Stefanini, S.; Zamparelli, C.; Theil, E. C.; Chiancone, E. *J. Biol. Chem.* **2009**, *284*, 19101−19109.
(49) Lawson, D. M.; Treffry, A.; Artymiuk, P. J.; Harrison, P. M.; Yewdall, S. J.; Luzzago, A.; Cesareni, G.; Levi, S.; Arosio, P. *FEBS Lett.* **1989**, *254*, 207−210.
(50) Ha, Y.; Shi, D.; Small, G. W.; Theil, E. C.; Allewell, N. M. *J. Biol. Inorg. Chem.* **1999**, *4*, 243−256.
(51) Bertini, I.; Lalli, D.; Mangani, S.; Pozzi, C.; Rosa, C.; Theil, E. C.; Turano, P. *J. Am. Chem. Soc.* **2012**, *134*, 6169−6176.
(52) Ceci, P.; Di Cecca, G.; Falconi, M.; Oteri, F.; Zamparelli, C.; Chiancone, E. *J. Biol. Inorg. Chem.* **2011**, *16*, 869−880.
(53) Calhoun, L. N.; Kwon, Y. M. *J. Appl. Microbiol.* **2011**, *110*, 375−386.
(54) Gauss, G. H.; Benas, P.; Wiedenheft, B.; Young, M.; Douglas, T.; Lawrence, C. M. *Biochemistry* **2006**, *45*, 10815−10827.
(55) Cairo, G.; Rappocciolo, E.; Tacchini, L.; Schiaffonati, L. *Biochem. J.* **1991**, *275* (Pt 3), 813−816.
(56) Levi, S.; Santambrogio, P.; Cozzi, A.; Rovida, E.; Corsi, B.; Tanborini, E.; Spada, S.; Albertini, A.; Arosio, P. *J. Mol. Biol.* **1994**, *238*, 649−654.
(57) Theil, E. C.; Small, G. W.; He, L.; Tipton, A.; Danger, D. *Inorg. Chim. Acta* **2000**, *297*, 242−251.
(58) Bou-Abdallah, F.; Biasiotto, G.; Arosio, P.; Chasteen, N. D. *Biochemistry* **2004**, *43*, 4332−4337.
(59) Mann, S. *Nat. Mater.* **2009**, *8*, 781−792.
(60) Yamashita, I.; Iwahori, K.; Kumagai, S. *Biochim. Biophys. Acta* **2010**, *1800*, 846−857.
(61) Terashima, M.; Uchida, M.; Kosuge, H.; Tsao, P. S.; Young, M. J.; Conolly, S. M.; Douglas, T.; McConnell, M. V. *Biomaterials* **2011**, *32*, 1430−1437.
(62) Kitagawa, T.; Kosuge, H.; Uchida, M.; Dua, M. M.; Iida, Y.; Dalman, R. L.; Douglas, T.; McConnell, M. V. *Mol. Imaging Biol.* **2012**, *14*, 315−324.
(63) Theil, E. C.; Behera, R. K. B. *The Chemistry of Nature's Iron Biominerals in Ferritin Protein Cages*; John Wiley & Sons: New York, 2013; Vol. *1*.
(64) Jameson, G. N. L.; Jin, W.; Krebs, C.; Perreira, A. S.; Tavares, P.; Liu, X.; Theil, E. C.; Huynh, B. H. *Biochemistry* **2002**, *41*, 13435−13443.
(65) Funk, F.; Lenders, J. P.; Crichton, R. R.; Schneider, W. *Eur. J. Biochem.* **1985**, *152*, 167−172.
(66) Takagi, H.; Shi, D.; Ha, Y.; Allewell, N. M.; Theil, E. C. *J. Biol. Chem.* **1998**, *273*, 18685−18688.
(67) Anderson, C. P.; Shen, M.; Eisenstein, R. S.; Leibold, E. A. *Biochim. Biophys. Acta* **2012**, *1823*, 1468−1483.
(68) Goss, D. J.; Theil, E. C. *Acc. Chem. Res.* **2011**, *44*, 1320−8.
(69) Iwasaki, K.; Mackenzie, E. L.; Hailemariam, K.; Sakamoto, K.; Tsuji, Y. *Mol. Cell. Biol.* **2006**, *26*, 2845−2856.
(70) Hintze, K. J.; Katoh, Y.; Igarashi, K.; Theil, E. C. *J. Biol. Chem.* **2007**, *282*, 34365−34371.
(71) Berdoukas, V.; Farmaki, K.; Carson, S.; Wood, J.; Coates, T. *J. Blood Med.* **2012**, *3*, 119−129.
(72) Vaisman, B.; Meyron-Holtz, E. G.; Fibach, E.; Krichevsky, A. M.; Konijn, A. M. *Br. J. Hamaetol.* **2000**, *110*, 394−401.
(73) Davila-Hicks, P.; Theil, E. C.; Lonnerdal, B. *Am. J. Clin. Nutr.* **2004**, *80*, 936−940.
(74) Leimberg, M. J.; Prus, E.; Konijn, A. M.; Fibach, E. *J. Cell. Biochem.* **2008**, *103*, 1211−1218.
(75) Theil, E. C.; Chen, H.; Miranda, C.; Janser, H.; Elsenhans, B.; Nunez, M. T.; Pizarro, F.; Schumann, K. *J. Nutr.* **2012**, *142*, 478−483.
(76) Burton, J. W.; Harlow, C.; Theil, E. C. *J. Plant Nutr.* **1998**, *21*, 913−927.

(77) Lynch, S. R.; Beard, J. L.; Dassenko, S. A.; Cook, J. D. *Am. J. Clin. Nutr.* **1984**, *40*, 42−47.
(78) Beard, J. L.; Burton, J. W.; Theil, E. C. *J. Nutr.* **1996**, *126*, 154−160.
(79) Murray-Kolb, L. E.; Welch, R.; Theil, E. C.; Beard, J. L. *Am. J. Clin. Nutr.* **2003**, *77*, 180−184.
(80) Martinez Meyer, M. R.; Rojas, A.; Santanen, A.; Stoddard, F. L. *Food Chem.* **2013**, *136*, 87−93.
(81) Mertz, J. R.; Theil, E. C. *J. Biol. Chem.* **1983**, *258*, 11719−11726.
(82) Treffry, A.; Harrison, P. M. *Biochem. J.* **1984**, *220*, 357−859.
(83) De Domenico, I.; Vaughn, M. B.; Li, L.; Bagley, D.; Musci, G.; Ward, D. M.; Kaplan, J. *EMBO J.* **2006**, *25*, 5396−5404.
(84) Theil, E. C.; Goss, D. J. *Chem. Rev.* **2009**, *109*, 4568−4579.
(85) Darbani, B.; Briat, J. F.; Holm, P. B.; Husted, S.; Noeparvar, S.; Borg, S. *Biotechnol. Adv.* **2013**.
(86) Ferreira, F.; Bucchini, D.; Martin, M. E.; Levi, S.; Arosio, P.; Grandchamp, B.; Beaumont, C. *J. Biol. Chem.* **2000**, *275*, 3021−3024.
(87) Dehner, C.; Morales-Soto, N.; Behera, R. K.; Shrout, J.; Theil, E. C.; MAurice, P. A.; Dubois, J. L. *J. Biol. Inorg. Chem.* **2013**, *18*, 371−381.
(88) Oshtrakh, M. I.; Alenkina, I. V.; Vinogradov, A. V.; Konstantinova, T. S.; Kuzmann, E.; Semionkin, V. A. *Biometals* **2013**, *26*, 229−239.
(89) Zuyderhoudt, F. M.; Sindram, J. W.; Marx, J. J.; Jorning, G. G.; van Gool, J. *Hepatology* **1983**, *3*, 232−235.
(90) Luten, M.; Roerdinkholder-Stoelwinder, B.; Rombout-Sestrienkova, E.; de Grip, W. J.; Bos, H. J.; Bosman, G. J. *Transfusion* **2008**, *48*, 436−441.
(91) Musallam, K. M.; Cappellini, M. D.; Taher, A. T. *Curr. Opin. Hematol.* **2013**, *20*, 187−192.
(92) Trachtenberg, F.; Vichinsky, E.; Haines, D.; Pakbaz, Z.; Mednick, L.; Sobota, A.; Kwiatkowski, J.; Thompson, A. A.; Porter, J.; Coates, T.; Giardina, P. J.; Olivieri, N.; Yamashita, R.; Neufeld, E. J. *Am. J. Hematol.* **2011**, *86*, 433−436.
(93) De Domenico, I.; Ward, D. M.; Kaplan, J. *Blood* **2009**, *114*, 4546−4551.
(94) Tibodeau, J. D.; Fox, P. M.; Ropp, P. A.; Theil, E. C.; Thorp, H. H. *Proc. Natl. Acad. Sci. U. S. A.* **2006**, *103*, 253−257.
(95) Melefors, O.; Goossen, B.; Johansson, H. E.; Stripecke, R.; Gray, N. K.; Hentze, M. W. *J. Biol. Chem.* **1993**, *268*, 5974−5978.
(96) Bennett, T. M.; Maraini, G.; Jin, C.; Sun, W.; Hejtmancik, J. F.; Shiels, A. *Mol. Vis.* **2013**, *19*, 835−844.
(97) Uchida, M.; Kang, S.; Reichhardt, C.; Harlen, K.; Douglas, T. *Biochim. Biophys. Acta* **2010**, *1800*, 834−845.
(98) San Martin, C. D.; Garri, C.; Pizarro, F.; Walter, T.; Theil, E. C.; Nunez, M. T. *J. Nutr.* **2008**, *138*, 659−666.
(99) Han, J.; Seaman, W. E.; Di, X.; Wang, W.; Willingham, M.; Torti, F. M.; Torti, S. V. *PLoS One* **2011**, *6*, e23800.
(100) Leung, K., 2004.
(101) Uchida, M.; Terashima, M.; Cunningham, C. H.; Suzuki, Y.; Willits, D. A.; Willis, A. F.; Yang, P. C.; Tsao, P. S.; McConnell, M. V.; Young, M. J.; Douglas, T. *Magn. Reson. Med.* **2008**, *60*, 1073−1081.
(102) Antileo, E.; Garri, C.; Tapia, V.; Munoz, J. P.; Chiong, M.; Nualart, F.; Lavandero, S.; Fernandez, J.; Nunez, M. T. *Am. J. Physiol. Gastrointest. Liver Physiol.* **2013**, *304*, G655−G661.
(103) Pasricha, S. R.; Drakesmith, H.; Black, J.; Hipgrave, D.; Biggs, B. A. *Blood* **2013**.
(104) Ragland, M.; Theil, E. C. *Plant Mol. Biol.* **1993**, *21*, 555−560.
(105) Theil, E. C.; Hase, T. Plant and microbial ferritins. In *Iron Chelation in Plants and Soil Microorganisms*; Academic Press: San Diego, 1993; pp 133−156.
(106) Theil, E. C. Red cell ferritin and iron storage during the early hemoglobin switch. In *Hemoglobins in Development and Differentiation*; Stamatoyannopoulos, G., Nienhuis, A., Eds.; Alan R. Liss, Inc.: New York, 1981; pp 423−431.
(107) Munro, H. N.; Linder, M. C. *Physiol. Rev.* **1978**, *58*, 318−396.
(108) Li, J.; Shiraki, T.; Igarashi, K. *Commun. Integr. Biol.* **2013**, *5*, 477−479.